Higher key rate practical twin field quantum key distribution through sending or not sending

Cong Jiang¹, Xiao-Long Hu¹, Hai Xu¹, Zong-Wen Yu^{1,3} and Xiang-Bin Wang^{1,2,4,5*†}

¹State Key Laboratory of Low Dimensional Quantum Physics, Department of Physics,

Tsinghua University, Beijing 100084, China

² Synergetic Innovation Center of Quantum Information and Quantum Physics,

University of Science and Technology of China, Hefei, Anhui 230026, China

³Data Communication Science and Technology Research Institute, Beijing 100191, China

⁴ Jinan Institute of Quantum technology, SAICT, Jinan 250101, China

⁵ Shenzhen Institute for Quantum Science and Engineering, and Physics Department,

Southern University of Science and Technology, Shenzhen 518055, China

The sending-or-not-sending (SNS) protocol of the twin-field quantum key distribution (TF-QKD) has its advantage of unconditional security proof under whatever coherent attack and fault tolerance to large misalignment error, and hence has attracted lots of attentions. In this paper, we study the finite key effect of SNS protocol with two way communication and obtain the key rate formula by taking all the finite key effect into consideration. Besides, we show how to apply our method to the asymmetric SNS protocol. The numerical results show that in the case of finite key size, our method can greatly improve the key rate of SNS protocol with both symmetric channel and asymmetric channel, and unconditionally break the absolute key rate limit of repeater-less quantum key distribution. Comparison shows that the simulated key rates presented here are the best known results of practical QKD.

I. INTRODUCTION

In 1984, Bennett and Brassard proposed the first quantum key distribution (QKD) protocol, BB84 protocol [1], which can provide the unconditional secure private communication between Alice and Bob [1–8]. But the security of BB84 protocol cannot be guaranteed given imperfect devices such as the weak coherent state (WCS) source or the imperfect detectors such as avalanche photodiode detectors (APDs) are used [9–17]. The decoy-state method [18–20] can assure the security of the OKD protocol with imperfect sources and maintain the high key rate, and thus attracts many studies on both the theories [21–28] and experiments [29–39]. Besides decov-state mehtod, there are other protocols such as RRDPS protocol [40, 41] proposed to beat photonnumber-splitting (PNS) attack. Measurement-Device-Independent (MDI)-QKD [42, 43] was proposed to solve all possible detection loopholes. The decoy-state MDI-QKD can assure the security with imperfect sources and detectors, and thus has been widely studied [44–57].

Recently a protocol named Twin-Field (TF)QKD [58] was proposed, changing the key rate into square root scale of channel transmittance. The protocol can break the repeater-less key-rate limit such as the famous TGW bound [59] and the PLOB bound [60] which will be used in this work. Later, many variants [61–74] of TFQKD were proposed to close the security loophole due to the

post announced phase information. Experiments [75–79] have been done to demonstrate those protocols. In particular, an efficient protocol named sending-or-not-sending (SNS) protocol has been proposed in Ref. [61]. The SNS protocol has its advantage of tolerating large misalignment errors [61, 67] and unconditional security with finite pulses [70]. The numerical results show that the secure distance can exceed 500~km even when the misalignment error is as large as 20% [70]. The SNS protocol has been experimentally demonstrated in proof-of-principle in Ref. [75], and realized in real optical fiber with the finite key effects being taken into consideration [76].

However, there are still considerable spaces to further improve the practical feasibility of the SNS protocol. First, the original SNS protocol [61, 67, 70] is limited to small probability of sending a signal coherent state. Second, the original SNS protocol is limited to the symmetric source parameters for Alice and Bob while we need to use asymmetric source parameters given asymmetric channel in practice.

The two way communication method, actively odd-parity pairing (AOPP) can be used to SNS protocol to thus increase the probability of sending the signal coherent state [71]. The key rate of SNS protocol with AOPP is about twice that of original SNS protocol in the case of infinite pulses and infinite intensities [71]. However, there are only finite pulses and finite intensities in practice, thus we need to consider the effect of finite key size. In this article, we study the complete effect of finite key size including the statistical fluctuation, the finite intensities, the finite phase slice, and the composable security. And we compare the results with the original SNS protocol with the complete effect of finite key size to see whether

^{*}Email Address: xbwang@mail.tsinghua.edu.cn

 $^{^\}dagger Also$ at Center for Atomic and Molecular Nanosciences, Tsinghua University, Beijing 100084, China

the advantages of the improved scheme still hold. As a result, we find that the advantage of AOPP [71] is still there. More extensive comparisons among different protocols show that the key-rate results simulated in this work from AOPP present the highest key rate known so far, if we assume a reasonable finite size of the key.

To apply SNS protocol efficiently over assymetric channel where the distance between Alice and Charlie differs significantly from that of Bob and Charlie, we need consider the asymmetric SNS protocol [72]. In this paper, we also show how to apply our method to the asymmetric SNS protocol.

Breaking the repeater-less key-rate limit is the most fascinating property of the TF-QKD. In practice, there are lot of constraints. We set the following conditions for practical QKD results that unconditionally break the repeater-less key rate limit:

- 1. The protocol itself must be secure.
- 2. A reasonable finite size of the key should be assumed and the finite key effects should be considered in calculation.
- 3. The actual key rate should break the absolute PLOB bound [80], which upper bounds the repeater-less key rate given whatever local devices, including the perfect detection devices.

For this goal, we need to consider the finite key effects and we need to show a high key rate exceeding the absolute PLOB bound.

The composable security coefficient is the security criterion of the universally composable framework [81]. In the end of a QKD protocol, Alice gets a key string K, and Bob gets a key string K'. A protocol is called ε_{cor} -correct if the probability that K and K' aren't the same is no larger than ε_{cor} , $\Pr(K \neq K') \leq \varepsilon_{cor}$.

Besides, the protocol may be attacked by Eve and some information would be leaked to Eve. We denote the density operator of the system of Alice and Eve as ρ_{AE} . If

$$\min_{\rho_E} \frac{1}{2} \parallel \rho_{AE} - U_A \otimes \rho_E \parallel \leq \varepsilon_{sec}, \tag{1}$$

where U_A denotes the fully mixed state of Alice's system and ρ_E is the density operator of Eve's system, the protocol is called ε_{sec} -secret [53, 82, 83]. According to the composable framework, a protocol is called ε -secure if it is both ε_{cor} -correct and ε_{sec} -secret, and $\varepsilon_{cor} + \varepsilon_{sec} \leq \varepsilon$.

This paper is arranged as follows. In Sec. II, we introduce the content of 4-intensities SNS protocol and the main results of the effect of finite key size. In Sec. III, we show how to apply our method to asymmetric SNS protocol. And in Sec. IV, we present our numerical simulation results. The article ends with some concluding remarks. The details of calculation are shown in the appendix.

II. THE FINITE KEY EFFECT OF SNS PROTOCOL WITH AOPP

In practice, there are only finite intensities, and we consider the 4-intensity SNS protocol, where each sides will use 4 different intensities. In this protocol, Alice and Bob each prepare a vacuum pulse or phase-randomized WCS pulse with intensity randomly chosen from the 3 different values and send them to an untrusted party, Charlie. Charlie is assumed to perform interferometric measurements on the received pulses and announces the measurement results to Alice and Bob. Alice and Bob repeat this process for N times and get a series of data. Finally, Alice and Bob can extract the secure final keys from those data according to the key rate formula. The preparation and measurement processes of this protocol are the same with that of Ref. [70]. The details of the protocol are shown as follows.

The preparation and measurement. In each time window, Alice (Bob) randomly chooses the decoy window or signal window with probabilities $1 - p_z$ and p_z respectively. If the decoy window is chosen, Alice (Bob) randomly prepares the pulse of state $|0\rangle$, $|e^{i\theta_A}\sqrt{\mu_1}\rangle$ or $|e^{i\theta'_A}\sqrt{\mu_2}\rangle$ (state $|0\rangle$, $|e^{i\theta_B}\sqrt{\mu_1}\rangle$ or $|e^{i\theta'_B}\sqrt{\mu_2}\rangle$) with probabilities p_0 , p_1 and $1-p_0-p_1$, respectively, where $\theta_A, \theta_A', \theta_B$ and θ_B' are different in different windows, and are random in $[0, 2\pi)$. If the signal window is chosen, Alice (Bob) randomly chooses bit 1 or 0 (0 or 1) with probabilities ϵ and $1-\epsilon$, respectively. If bit 1 (0) is chosen, Alice (Bob) prepares a phase-randomized WCS pulse with intensity μ_z . If bit 0 (1) is chosen, Alice (Bob) prepares a vacuum pulse. Then Alice and Bob send their prepared pulses to Charlie. Charlie is assumed to perform interferometric measurements on the received pulses and announces the measurement results to Alice and Bob. If one and only one detector clicks in the measurement process, Charlie also tells Alice and Bob which detector clicks, and Alice and Bob take it as an one-detector heralded event. Alice and Bob repeat the above process for N times and collect all the data with one-detector heralded events and discard all the others.

The next process is the data post processing. To clearly show how this process is carried out, we have the following definitions.

Definition 1. If both Alice and Bob choose the signal window, it is a Z window. If both Alice and Bob choose the decoy window, Alice chooses to prepare the pulse of state $|e^{i\theta_A}\sqrt{\mu_1}\rangle$, and Bob chooses to prepare the pulse of state $|e^{i\theta_B}\sqrt{\mu_1}\rangle$, and θ_A and θ_B satisfy

$$1 - |\cos(\theta_A - \theta_B - \psi_{AB})| \le \lambda, \tag{2}$$

it is an X window. Here ψ_{AB} can take an arbitrary value which can be different from time to time as Alice and Bob like, so as to obtain a satisfactory key rate for the protocol [76]. If there are infinite pulses in the protocol, λ can be infinitely close to 0. But in practice, λ is an finite small value. The one-detector heralded events of

X windows and Z windows are called effective events. And Alice and Bob respectively get n_t -bit strings, Z_A and Z_B , formed by the corresponding bits of effective events of Z windows.

Definition 2. For an effective event in the Z windows, if it is caused by the event that only one party of Alice and Bob decides sending out a phase-randomized WCS pulse and he (she) actually sends out a single photon state from the view point of decoy state method, it is an untagged event. Its corresponding bit is an untagged bit.

Parameter estimation. We define n_t as the number of effective events of Z windows, E_z as the bit-flip error rate of strings Z_A and Z_B . And the data of all the one-detector heralded events except the effective events of Z windows in this protocol are used to estimate the expected value of the lower bounds of the number of untagged 0-bits, $\langle \underline{n_{01}} \rangle$, and untagged 1-bits, $\langle \underline{n_{10}} \rangle$. The details of how to estimate the lower bound of $\langle \underline{n_{01}} \rangle$ and $\langle n_{10} \rangle$ are shown in the appendix.

Besides, we need to estimate the expected value of the upper bound of phase flip error rate, $\langle \overline{e_1^{ph}} \rangle$, of the untagged events. The error counting rate of the X windows, T_X can be used to estimate $\langle \overline{e_1^{ph}} \rangle$. The error events in X windows are defined as follows: the phases of the pulse pair in the X windows satisfy $\cos(\theta_A - \theta_B) > 0$ and Charlie announces that this pulse pair causes the right detector clicking, or the phases of the pulse pair in the X windows satisfy $\cos(\theta_A - \theta_B) < 0$ and Charlie announces that this pulse pair causes the left detector clicking. We denote the number of total pulses send out in the X windows as N_X , and the number of error events in the X windows as M_X , then we have

$$T_X = \frac{m_X}{N_X}. (3)$$

aborts.

The calculation details of how to estimate $\langle \overline{e_1^{ph}} \rangle$ are shown in the appendix.

Error correction preprocessing. AOPP is a twoway communication method to refine the structure of bitflip error of Alice's and Bob's bit strings [71]. In AOPP process, Bob combines the bits in Z_B two by two, and obtains a series of pairs. In each pair, one bit is randomly chosen from all the bits 0, and the other bit is randomly chosen from all the bits 1. As the numbers of the bits 0 and the bits 1 in Z_B are always not the same, if there are n_{t0} bits 0 and n_{t1} bits 1, Bob finally obtains $n_p =$ $\min(n_{t0}, n_{t1})$ pairs. The unpaired bits would be directly discarded. Here we use notation (i, j) for the bit pair that contains i-th and j-th bit from \mathbb{Z}_B , and the corresponding bit values are z_i and z_j . Then Bob broadcasts (i, j) and $z_i \oplus z_j$ to Alice. Alice calculates the value of $z_i' \oplus z_j'$, where z'_i is the value of i-th bit and z'_i is the value of j-th bit of \vec{z}_A . If $z_i \oplus z_j \neq z_i' \oplus z_j'$, Alice and Bob discard this bit pair; If $z_i \oplus z_j = z_i' \oplus z_j'$, Alice and Bob keep the second bit of the bit pair. The remained bits of Alice and Bob form two new n'_t -bit strings Z'_A and Z'_B .

The untagged bits now are the bits that survived from the bit pair formed by two untagged bits. And we can estimate the expected value of the lower bound of the number of those new untagged bits, $\langle \underline{n'_1} \rangle$, according to $\langle n_{01} \rangle$ and $\langle n_{10} \rangle$, which is

$$\langle \underline{n_1'} \rangle = \frac{\langle \underline{n_{01}} \rangle}{n_{t0}} \frac{\langle \underline{n_{10}} \rangle}{n_{t1}} n_p. \tag{4}$$

The phase-flip error rate of those new untagged bits is $\langle \overline{e_1^{ph\prime}} \rangle = 2 \langle \overline{e_1^{ph}} \rangle (1 - \langle \overline{e_1^{ph}} \rangle)$ [71].

We can use the Chernoff bound to help us estimate the real value of the number of new untagged bits and the corresponding phase flip error rate with Eqs. (A13)-(A16), which are

$$n_1' = \varphi^L(\langle \underline{n_1'} \rangle), \quad e_1^{ph} = \frac{\varphi^U(\langle \underline{n_1'} \rangle \langle \overline{e_1^{ph'}} \rangle)}{\langle \underline{n_1'} \rangle},$$
 (5)

where $\varphi^L(x)$ and $\varphi^U(x)$ are defined in Eqs. (A13)-(A16). **Error correction and privacy amplification.** Alice and Bob perform an information reconciliation scheme to correct Z_B' , and Bob will obtain an estimated \hat{Z}_A' of Z_A' from Z_B' . To make sure the error correction scheme is successfully performed, Alice computes a hash of Z_A' of length $\log_2(1/\varepsilon_{cor})$ using a random universal hash function, and she sends the hash and hash function to Bob [84]. If the hash that Bob computes is the same with Alice, the probability that Z_A' and \hat{Z}_A' aren't the same, $\Pr(Z_A' \neq \hat{Z}_A')$, is less than ε_{cor} . If the hash that Bob computes is not the same with Alice, the protocol

Then Alice and Bob apply a privacy amplification scheme based on two-universal hashing [84] to extract two shorter strings to meet the criterion of Eq. (1). As we have known the lower bound of the number of the new untagged bits and the upper bound of the phase flip error rate of those new untagged bits, and decoy state method used here is the same as that of Ref. [70], we can directly use the formula of key rate with finite key effect in Ref. [70] to calculate the length of final keys

$$l_A = n_1'[1 - h(e_1^{ph'})] - f n_t' h(E_Z') - \log_2 \frac{2}{\varepsilon_{cor}} - 2\log_2 \frac{1}{\sqrt{2}\varepsilon_{PA}\hat{\varepsilon}},$$

$$(6)$$

where E_Z' is the bit flip error rate of strings Z_A' and Z_B' . With the formula of Eq. (6), the protocol is ε_{tol} -secure, and $\varepsilon_{tol} = \varepsilon_{cor} + \varepsilon_{sec}$, where $\varepsilon_{sec} = 2\hat{\varepsilon} + 4\bar{\varepsilon} + \varepsilon_{PA} + \varepsilon_{n_1'}$. Here, $\bar{\varepsilon}$ is the failure probability for the estimation of phase flip error rate of untagged bits in strings Z_A' and Z_B' , i.e., the probability that the real value of phase-flip error rate of untagged bits is larger than $e_1^{ph'}$; $\varepsilon_{n_1'}$ is the failure probability for the estimation of the lower bound of the number of untagged bits in strings Z_A' and Z_B' , i.e., the probability that the real value of the number of new untagged bits is smaller than n_1' , and ε_{PA} is the failure probability of privacy amplification.

III. THE ASYMMETRIC SNS PROTOCOL WITH AOPP AND FINITE KEY EFFECT

In the practical application of SNS protocol, the distance between Alice and Charlie can be different from the distance between Bob and Charlie. To solve this problem, the theory of asymmetric SNS protocol is proposed in Ref. [72]. The preparation and measurement step of asymmetric SNS protocol is the same with that of the original SNS protocol, except the source parameters of Alice and Bob in asymmetric SNS protocol are not the same. In this part, we use the subscript ' to indicate Bob's source parameters. For example, p_z is the probability that Alice chooses the signal window and p'_z is the probability that Bob chooses the signal window; μ_z is the intensity of phase-randomized WCS if Alice chooses to send out an unvacuum state in her signal windows and μ'_z is the intensity of phase-randomized WCS if Bob chooses to send out an unvacuum state in his signal windows.

Note that the original SNS protocol [61] and its improved one [71] based on symmetric source parameters for Alice and Bob, i.e., they use the same values for the sending probabilities and light intensities. As was shown in Ref. [72], the SNS protocol is also secure with asymmetric source parameters given the following mathematical constraint:

$$\frac{\mu_1}{\mu_1'} = \frac{\epsilon(1 - \epsilon')\mu_z e^{-\mu_z}}{\epsilon'(1 - \epsilon)\mu_z' e^{-\mu_z'}}.$$
 (7)

With this condition, light intensity chosen by Alice and that chosen by Bob can be different.

After Alice and Bob repeat the preparation and measurement steps of asymmetric SNS protocol for N times, they can perform the same error correction preprocessing, the error correction and privacy amplification steps as shown in Sec. II. And the formula of key rate is the same as Eq. (6). The major differences between the original SNS protocol and asymmetric SNS protocol are the forms of the formulas of the lower bound of the number of untagged bits and the upper bound of phase flip error rate, which are shown in the appendix.

IV. NUMERICAL SIMULATION

In this part, we show the results of numerical simulation of SNS protocol with AOPP, including the symmetric and asymmetric cases, and compare with the results of the original SNS protocol [70, 72].

We use the linear model to simulate the observed values of experiment with the experimental parameters list in Table. I. Without loss of generality, we assume the property of Charlie's two detectors are the same. The distance between Alice and Charlie is L_A , and the distance between Bob and Charlie is L_B . The total distance between Alice and Bob is $L = L_A + L_B$. In our numerical

p_d	e_d	η_d	f	α_f	ξ
1.0×10^{-8}	3%	30.0%	1.1	0.2	1.0×10^{-10}

TABLE I: List of experimental parameters used in numerical simulations. Here p_d is the dark count rate of Charlie's detectors; e_d is the misalignment-error probability; η_d is the detection efficiency of Charlie's detectors; f is the error correction inefficiency; α_f is the fiber loss coefficient (dB/km); ξ is the failure probability of statistical fluctuation analysis.

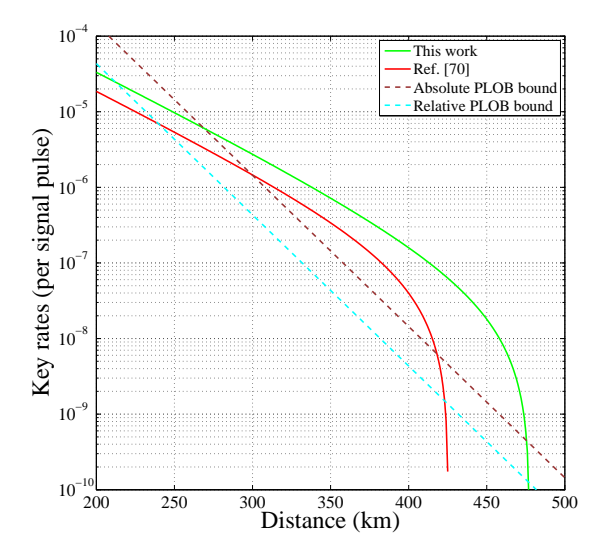


FIG. 1: The optimal key rates (per pulse) versus transmission distance (the distance between Alice and Bob) with total number of pulses $N=10^{12}$. Here we set $L_A=L_B$ and the source parameters of Alice and Bob are all the same. The experimental parameters that we used in the numerical simulation are listed in Table I. the green solid line is the optimized results of this work. And the red solid line is the optimized results of Ref. [70]. The absolute PLOB bound is calculated by the formula presented in Ref. [80], which bounds the key rate of repeater-less QKD with whatever devices, such as perfect detection device. Relative PLOB bound assumes a limited detection efficiency as listed in Table I.

simulation, we set $L_A = L_B$ for the symmetric case and $L_A - L_B = constant$ for the asymmetric case.

By setting the failure probability of Chernoff bound as ξ , we have $\bar{\varepsilon}=3\xi$ and $\varepsilon_{n_1'}=6\xi$, because we use the Chernoff bound for three times to estimate $e_1^{ph'}$ and we use the Chernoff bound for six times to estimate n_1' . And we set $\varepsilon_{cor}=\hat{\varepsilon}=\varepsilon_{PA}=\xi$, thus the security coefficients, $\varepsilon_{tol}=22\xi=2.2\times10^{-9}$.

Figure 1 and Figure 2 are our simulation results of this work and Ref. [70] with the experimental parameters list in Table. I. In Fig. 1 and Fig. 2, we set $L_A = L_B$ and the source parameters of Alice and Bob are all the same. The dashed brown lines in Fig. 1 and Fig. 2 are the results of absolute PLOB bound, which bounds the key

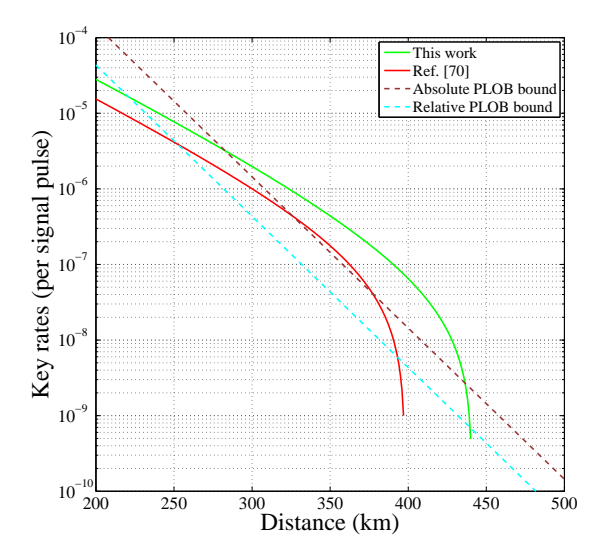


FIG. 2: The optimal key rates (per pulse) versus transmission distance with total number of pulses $N=10^{11}$. Here we set $L_A=L_B$ and the source parameters of Alice and Bob are all the same. The experimental parameters that we used in the numerical simulation are listed in Table I. The green solid line is the optimized results of this work. And the red solid line is the optimized results of Ref. [70].

rate of repeater-less QKD with whatever devices, such as perfect detection device. The cyan dashed lines are the results of relative PLOB bound, which assumes a limited detection efficiency as listed in Table I. The results show that our method can obviously exceed the absolute PLOB bound. We set $N=1.0\times10^{11}$ in Fig. 2, which is a more practical number of total pulse in experiment, and results show that our method still obviously exceeds the absolute PLOB bound, while the original SNS protocol just exceeds the absolute PLOB bound a little.

Figure 3 and Figure 4 are our simulation results of this work and Ref. [72] with the experimental parameters list in Table. I. In Fig. 3 and Fig. 4, we set $L_A - L_B = 100 km$. From Fig. 3 and Fig. 4, we can clearly see that the our method in the case of finite key size can greatly improved the key rate of SNS protocol with asymmetric channels, especially when the channel loss is large.

Table. II is the key rates of this work and Ref. [79]. We use the parameters of Ref. [79] in calculations, which are $p_d=3.36\times 10^{-8},\ e_d=7\%,\ \eta_d=20\%,\ \alpha_f=0.185,\ \xi=1.69\times 10^{-10},\$ and $N=2.0\times 10^{13}$ for the distance of 402 km, and $p_d=1.26\times 10^{-8},\ e_d=9.8\%,\ \eta_d=29\%,\ \alpha_f=0.162,\ \xi=1.71\times 10^{-10},\$ and $N=2.0\times 10^{13}$ for the distance of 502 km. The results in Table. II show that the key rates of this work are more than ten times that of Ref. [79].

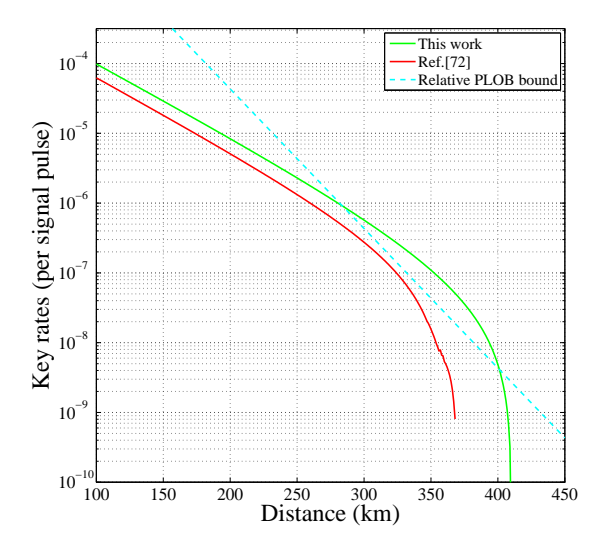


FIG. 3: The optimal key rates (per pulse) versus transmission distance with total number of pulses $N=10^{12}$. Here we set $L_A-L_B=100km$. The experimental parameters that we used in the numerical simulation are listed in Table I. The green solid line is the optimized results of this work. And The red green line is the optimized results of Ref. [72].

key rate	402km	502km
this work	1.05×10^{-7}	5.12×10^{-8}
Ref. [79]	1.44×10^{-8}	1.68×10^{-9}

TABLE II: The key rates of this work and Ref. [79]. We use the parameters of Ref. [79] in calculations, e.g., the dark count rate is $p_d=3.36\times 10^{-8}$, the misalignment-error probability is $e_d=7\%$, the detection efficiency is $\eta_d=20\%$, the fiber loss is $\alpha_f=0.185$, the failure probability is $\xi=1.69\times 10^{-10}$, and the total number pulse is $N=2.0\times 10^{13}$ for the distance of 402 km, and $p_d=1.26\times 10^{-8}$, $e_d=9.8\%$, $\eta_d=29\%$, $\alpha_f=0.162$, $\xi=1.71\times 10^{-10}$, and $N=2.0\times 10^{13}$ for the distance of 502 km.

V. CONCLUSION

In this paper, we study the secure key rate of SNS protocol with AOPP in the situation of finite key size. We consider all the finite key effect and get the formula of key rate as shown in Eq. (6). The numerical results show that AOPP can greatly improve the key rate of SNS protocol for both the asymmetric and symmetric channels, and unconditionally breaking the absolute key rate limit of repeater-less quantum key distribution. Our results can directly be used to the SNS experiments.

Acknowledgement: We acknowledge the financial support in part by Ministration of Science and Technology of China through The National Key Research and Development Program of China grant No. 2017YFA0303901; National Natural Science Foundation

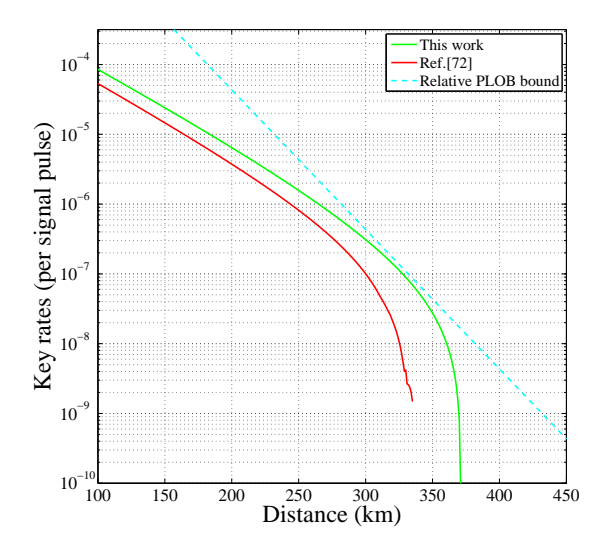


FIG. 4: The optimal key rates (per pulse) versus transmission distance with total number of pulses $N=10^{11}$. Here we set $L_A-L_B=100km$. The experimental parameters that we used in the numerical simulation are listed in Table I. The green solid line is the optimized results of this work. And The red green line is the optimized results of Ref. [72].

of China grant No. 11474182, 11774198 and U1738142.

Appendix A: The calculation method

The calculation methods of $\langle n_{01} \rangle$, $\langle n_{10} \rangle$, and $\langle e_1^{ph\prime} \rangle$ are similar with that in Refs [67, 70–72]. And the formulas of asymmetric SNS protocol are more general. We can easily get the formulas of original SNS protocol from that of asymmetric SNS protocol by setting the same source parameters of Alice and Bob, that is, drop the subscript ' in the formulas.

To clearly show the calculation method, we denote Alice's sources $|0\rangle$, $|e^{i\theta_A}\sqrt{\mu_1}\rangle$ and $|e^{i\theta'_A}\sqrt{\mu_2}\rangle$ as o, x, and y. Similarly, we denote Bob's sources $|0\rangle$, $|e^{i\theta_B}\sqrt{\mu'_1}\rangle$, and $|e^{i\theta'_B}\sqrt{\mu'_2}\rangle$ as o', x', and y'. We denote the number of pulse pairs of source $\alpha\beta(\alpha=o,x,y;\beta=o',x',y')$ sent out in the whole protocol as $N_{\alpha\beta}$, and the total number of one-detector heralded events of source $\alpha\beta$ as $n_{\alpha\beta}$. We define the counting rate of source $\alpha\beta$ as $s_{\alpha\beta}=n_{\alpha\beta}/N_{\alpha\beta}$, and the corresponding expected value as $s_{\alpha\beta}>0$. With all

those definitions, we have

$$N_{oo'} = \{(1 - p_z)[(1 - p_z')p_0p_0' + p_z'p_0(1 - \epsilon')] + p_z(1 - p_z')(1 - \epsilon)p_0'\}N$$

$$N_{ox'} = (1 - p_z')p_1'[(1 - p_z)p_0 + p_z(1 - \epsilon)]N$$

$$N_{xo'} = (1 - p_z)p_1[(1 - p_z')p_0' + p_z'(1 - \epsilon')]N$$

$$N_{oy'} = (1 - p_z)(1 - p_0' - p_1')[(1 - p_z)p_0 + p_z(1 - \epsilon)]N$$

$$N_{yo'} = (1 - p_z)(1 - p_0 - p_1)[(1 - p_z')p_0' + p_z'(1 - \epsilon')]N$$

$$N_{yo'} = (1 - p_z)(1 - p_0 - p_1)[(1 - p_z')p_0' + p_z'(1 - \epsilon')]N$$
(A1)

As sources x, y, x', y' are phase-randomized WCS sources, they are actually the classical mixture of different photon number states [72]. Thus we can use the decoy-state method to calculate the lower bounds of the expected values of the counting rate of states $|01\rangle\langle01|$ and $|10\rangle\langle10|$, which are

$$\langle \underline{s_{01}} \rangle = \frac{\mu_2'^2 e^{\mu_1'} \langle S_{ox'} \rangle - \mu_1'^2 e^{\mu_2'} \langle S_{oy'} \rangle - (\mu_2'^2 - \mu_1'^2) \langle S_{oo'} \rangle}{\mu_2' \mu_1' (\mu_2' - \mu_1')},$$

(A2)

$$\langle \underline{s_{10}} \rangle = \frac{\mu_2^2 e^{\mu_1} \langle S_{xo'} \rangle - \mu_1^2 e^{\mu_2} \langle S_{yo'} \rangle - (\mu_2^2 - \mu_1^2) \langle S_{oo'} \rangle}{\mu_2 \mu_1 (\mu_2 - \mu_1)}.$$
(A3)

Then we can get the lower bound of the expected value of the counting rate of untagged photons

$$\langle \underline{s_1} \rangle = \frac{\mu_1}{\mu_1 + \mu_1'} \langle \underline{s_{10}} \rangle + \frac{\mu_1'}{\mu_1 + \mu_1'} \langle \underline{s_{01}} \rangle, \quad (A4)$$

and

$$\langle n_{10} \rangle = N p_z p_z' \epsilon (1 - \epsilon') \mu_z e^{-\mu_z} \langle s_{10} \rangle,$$
 (A5)

$$\langle n_{01} \rangle = N p_z p_z' \epsilon' (1 - \epsilon) \mu_z' e^{-\mu_z'} \langle \underline{s_{01}} \rangle.$$
 (A6)

The upper bound of the expected value of e_1^{ph} is given by

$$\langle \overline{e_1^{ph}} \rangle = \frac{\langle T_X \rangle - e^{-\mu_1 - \mu_1'} \langle S_{oo'} \rangle / 2}{e^{-\mu_1 - \mu_1'} (\mu_1 + \mu_1') \langle \underline{s_1} \rangle}, \tag{A7}$$

where $\langle T_X \rangle$ is the expected value of T_X .

The Eqs.(A2)-(A7) are represented by expected values, but the values we get in experiment are observed values. To close the gap between the expected values and observed values, we need Chernoff bound [57, 85]. Let X_1, X_2, \ldots, X_n be n random samples, detected with the value 1 or 0, and let X denote their sum satisfying $X = \sum_{i=1}^{n} X_i$. ϕ is the expected value of X. We have

$$\phi^L(X) = \frac{X}{1 + \delta_1(X)},\tag{A8}$$

$$\phi^{U}(X) = \frac{X}{1 - \delta_2(X)},\tag{A9}$$

where we can obtain the values of $\delta_1(X)$ and $\delta_2(X)$ by solving the following equations

$$\left(\frac{e^{\delta_1}}{(1+\delta_1)^{1+\delta_1}}\right)^{\frac{X}{1+\delta_1}} = \frac{\xi}{2},\tag{A10}$$

$$\left(\frac{e^{-\delta_2}}{(1-\delta_2)^{1-\delta_2}}\right)^{\frac{X}{1-\delta_2}} = \frac{\xi}{2},\tag{A11}$$

where ξ is the failure probability. Thus we have

$$\phi^{L}(N_{\alpha\beta}S_{\alpha\beta}) = N_{\alpha\beta}\langle \underline{S}_{\alpha\beta}\rangle, \phi^{U}(N_{\alpha\beta}S_{\alpha\beta}) = N_{\alpha\beta}\langle \overline{S}_{\alpha\beta}\rangle.$$
(A12)

Besides, we can use the Chernoff bound to help us estimate their real values from their expected values. Similar to Eqs. (A8)- (A11), the observed value, φ , and its ex-

pected value, Y, satisfy

$$\varphi^{U}(Y) = [1 + \delta_1'(Y)]Y, \tag{A13}$$

$$\varphi^L(Y) = [1 - \delta_2'(Y)]Y, \tag{A14}$$

where we can obtain the values of $\delta'_1(Y)$ and $\delta'_2(Y)$ by solving the following equations

$$\left(\frac{e^{\delta_1'}}{(1+\delta_1')^{1+\delta_1'}}\right)^Y = \frac{\xi}{2},\tag{A15}$$

$$\left(\frac{e^{-\delta_2'}}{(1-\delta_2')^{1-\delta_2'}}\right)^Y = \frac{\xi}{2}.$$
 (A16)

- [1] C. H. Bennett and G. Brassard, in *Proceedings of the IEEE International Conference on Computers, Systems, and Signal Processing* (1984), pp. 175–179.
- [2] N. Gisin, G. Ribordy, W. Tittel, and H. Zbinden, Reviews of modern physics 74, 145 (2002).
- [3] N. Gisin and R. Thew, Nature photonics 1, 165 (2007).
- [4] V. Scarani, H. Bechmann-Pasquinucci, N. J. Cerf, M. Dušek, N. Lütkenhaus, and M. Peev, Reviews of modern physics 81, 1301 (2009).
- [5] P. W. Shor and J. Preskill, Physical review letters 85, 441 (2000).
- [6] M. Koashi, New Journal of Physics 11, 045018 (2009).
- [7] K. Tamaki, M. Koashi, and N. Imoto, Physical review letters 90, 167904 (2003).
- [8] B. Kraus, N. Gisin, and R. Renner, Physical review letters 95, 080501 (2005).
- [9] B. Huttner, N. Imoto, N. Gisin, and T. Mor, Physical Review A 51, 1863 (1995).
- [10] H. P. Yuen, Quantum and Semiclassical Optics: Journal of the European Optical Society Part B 8, 939 (1996).
- [11] G. Brassard, N. Lütkenhaus, T. Mor, and B. C. Sanders, Physical Review Letters 85, 1330 (2000).
- [12] N. Lütkenhaus, Physical Review A 61, 052304 (2000).
- [13] N. Lütkenhaus and M. Jahma, New Journal of Physics 4, 44 (2002).
- [14] L. Lydersen, C. Wiechers, C. Wittmann, D. Elser, J. Skaar, and V. Makarov, Nature photonics 4, 686 (2010).
- [15] I. Gerhardt, Q. Liu, A. Lamas-Linares, J. Skaar, C. Kurtsiefer, and V. Makarov, Nature communications 2, 349 (2011).
- [16] M. Hayashi, Physical Review A 76, 012329 (2007).
- [17] V. Scarani and R. Renner, Physical review letters 100, 200501 (2008).
- [18] W.-Y. Hwang, Physical Review Letters 91, 057901 (2003).
- [19] X.-B. Wang, Physical Review Letters 94, 230503 (2005).
- [20] H.-K. Lo, X. Ma, and K. Chen, Physical review letters 94, 230504 (2005).
- [21] X.-B. Wang, T. Hiroshima, A. Tomita, and M. Hayashi, Physics reports **448**, 1 (2007).
- [22] Y. Adachi, T. Yamamoto, M. Koashi, and N. Imoto, Physical review letters 99, 180503 (2007).

- [23] X.-B. Wang, C.-Z. Peng, and J.-W. Pan, Applied physics letters 90, 031110 (2007).
- [24] X.-B. Wang, C.-Z. Peng, J. Zhang, L. Yang, and J.-W. Pan, Physical Review A 77, 042311 (2008).
- [25] X.-B. Wang, L. Yang, C.-Z. Peng, and J.-W. Pan, New Journal of Physics 11, 075006 (2009).
- [26] K. Tamaki, M. Curty, G. Kato, H.-K. Lo, and K. Azuma, Physical Review A 90, 052314 (2014).
- [27] Z.-W. Yu, Y.-H. Zhou, and X.-B. Wang, Physical Review A 93, 032307 (2016).
- [28] H. F. Chau, Phys. Rev. A 97, 040301 (2018).
- [29] D. Rosenberg, J. W. Harrington, P. R. Rice, P. A. Hiskett, C. G. Peterson, R. J. Hughes, A. E. Lita, S. W. Nam, and J. E. Nordholt, Physical review letters 98, 010503 (2007).
- [30] T. Schmitt-Manderbach, H. Weier, M. Fürst, R. Ursin, F. Tiefenbacher, T. Scheidl, J. Perdigues, Z. Sodnik, C. Kurtsiefer, J. G. Rarity, et al., Physical Review Letters 98, 010504 (2007).
- [31] C.-Z. Peng, J. Zhang, D. Yang, W.-B. Gao, H.-X. Ma, H. Yin, H.-P. Zeng, T. Yang, X.-B. Wang, and J.-W. Pan, Physical review letters 98, 010505 (2007).
- [32] S.-K. Liao, W.-Q. Cai, W.-Y. Liu, L. Zhang, Y. Li, J.-G. Ren, J. Yin, Q. Shen, Y. Cao, Z.-P. Li, et al., Nature 549, 43 (2017).
- [33] M. Peev, C. Pacher, R. Alléaume, C. Barreiro, J. Bouda, W. Boxleitner, T. Debuisschert, E. Diamanti, M. Dianati, J. Dynes, et al., New Journal of Physics 11, 075001 (2009).
- [34] T.-Y. Chen, J. Wang, H. Liang, W.-Y. Liu, Y. Liu, X. Jiang, Y. Wang, X. Wan, W.-Q. Cai, L. Ju, et al., Optics express 18, 27217 (2010).
- [35] M. Sasaki, M. Fujiwara, H. Ishizuka, W. Klaus, K. Wakui, M. Takeoka, S. Miki, T. Yamashita, Z. Wang, A. Tanaka, et al., Optics express 19, 10387 (2011).
- [36] B. Fröhlich, J. F. Dynes, M. Lucamarini, A. W. Sharpe, Z. Yuan, and A. J. Shields, Nature 501, 69 (2013).
- [37] A. Boaron, G. Boso, D. Rusca, C. Vulliez, C. Autebert, M. Caloz, M. Perrenoud, G. Gras, F. Bussières, M.-J. Li, et al., Physical review letters 121, 190502 (2018).
- [38] Q. Wang, W. Chen, G. Xavier, M. Swillo, T. Zhang, S. Sauge, M. Tengner, Z.-F. Han, G.-C. Guo, and A. Karlsson, Physical Review Letters 100, 090501

- (2008).
- [39] F. Xu, Y. Zhang, Z. Zhou, W. Chen, Z. Han, and G. Guo, Physical Review A 80, 062309 (2009).
- [40] T. Sasaki, Y. Yamamoto, and M. Koashi, Nature 509, 475 (2014).
- [41] H. Takesue, T. Sasaki, K. Tamaki, and M. Koashi, Nature Photonics 9, 827 (2015).
- [42] S. L. Braunstein and S. Pirandola, Physical Review Letters 108, 130502 (2012).
- [43] H.-K. Lo, M. Curty, and B. Qi, Physical Review Letters 108, 130503 (2012).
- [44] X.-B. Wang, Physical Review A 87, 012320 (2013).
- [45] A. Rubenok, J. A. Slater, P. Chan, I. Lucio-Martinez, and W. Tittel, Physical Review Letters 111, 130501 (2013).
- [46] Y. Liu, T.-Y. Chen, L.-J. Wang, H. Liang, G.-L. Shentu, J. Wang, K. Cui, H.-L. Yin, N.-L. Liu, L. Li, et al., Physical Review Letters 111, 130502 (2013).
- [47] Z. Tang, Z. Liao, F. Xu, B. Qi, L. Qian, and H.-K. Lo, Physical Review Letters 112, 190503 (2014).
- [48] Y.-L. Tang, H.-L. Yin, S.-J. Chen, Y. Liu, W.-J. Zhang, X. Jiang, L. Zhang, J. Wang, L.-X. You, J.-Y. Guan, et al., Physical Review Letters 113, 190501 (2014).
- [49] C. Wang, X.-T. Song, Z.-Q. Yin, S. Wang, W. Chen, C.-M. Zhang, G.-C. Guo, and Z.-F. Han, Physical Review Letters 115, 160502 (2015).
- [50] L. Comandar, M. Lucamarini, B. Fröhlich, J. Dynes, A. Sharpe, S.-B. Tam, Z. Yuan, R. Penty, and A. Shields, Nature Photonics 10, 312 (2016).
- [51] H.-L. Yin, T.-Y. Chen, Z.-W. Yu, H. Liu, L.-X. You, Y.-H. Zhou, S.-J. Chen, Y. Mao, M.-Q. Huang, W.-J. Zhang, et al., Physical Review Letters 117, 190501 (2016).
- [52] C. Wang, Z.-Q. Yin, S. Wang, W. Chen, G.-C. Guo, and Z.-F. Han, Optica 4, 1016 (2017).
- [53] M. Curty, F. Xu, W. Cui, C. C. W. Lim, K. Tamaki, and H.-K. Lo, Nature communications 5, 3732 (2014).
- [54] F. Xu, H. Xu, and H.-K. Lo, Physical Review A 89, 052333 (2014).
- [55] Z.-W. Yu, Y.-H. Zhou, and X.-B. Wang, Physical Review A 91, 032318 (2015).
- [56] Y.-H. Zhou, Z.-W. Yu, and X.-B. Wang, Physical Review A 93, 042324 (2016).
- [57] C. Jiang, Z.-W. Yu, and X.-B. Wang, Physical Review A 95, 032325 (2017).
- [58] M. Lucamarini, Z. L. Yuan, J. F. Dynes, and A. J. Shields, Nature 557, 400 (2018).
- [59] M. Takeoka, S. Guha, and M. M. Wilde, Nature communications 5, 5235 (2014).
- [60] S. Pirandola, R. García-Patrón, S. L. Braunstein, and S. Lloyd, Physical review letters 102, 050503 (2009).
- [61] X.-B. Wang, Z.-W. Yu, and X.-L. Hu, Physical Review A 98, 062323 (2018).
- [62] K. Tamaki, H.-K. Lo, W. Wang, and M. Lucamarini, arXiv preprint arXiv:1805.05511 (2018).

- [63] X. Ma, P. Zeng, and H. Zhou, Physical Review X 8, 031043 (2018).
- [64] J. Lin and N. Lütkenhaus, Physical Review A 98, 042332 (2018).
- [65] C. Cui, Z.-Q. Yin, R. Wang, W. Chen, S. Wang, G.-C. Guo, and Z.-F. Han, Physical Review Applied 11, 034053 (2019).
- [66] M. Curty, K. Azuma, and H.-K. Lo, arXiv preprint arXiv:1807.07667 (2018).
- [67] Z.-W. Yu, X.-L. Hu, C. Jiang, H. Xu, and X.-B. Wang, Scientific Reports 9, 3080 (2019).
- [68] K. Maeda, T. Sasaki, and M. Koashi, Nature communications 10, 3140 (2019).
- [69] F.-Y. Lu, Z.-Q. Yin, C.-H. Cui, G.-J. Fan-Yuan, S. Wang, D.-Y. He, W. Chen, G.-C. Guo, and Z.-F. Han, arXiv preprint arXiv:1901.04264 (2019).
- [70] C. Jiang, Z.-W. Yu, X.-L. Hu, and X.-B. Wang, Physical Review Applied 12, 024061 (2019).
- [71] H. Xu, Z.-W. Yu, C. Jiang, X.-L. Hu, and X.-B. Wang, arXiv preprint arXiv:1904.06331 (2019).
- [72] X.-L. Hu, C. Jiang, Z.-W. Yu, and X.-B. Wang, arXiv preprint arXiv:1908.05073 (2019).
- [73] C.-H. Zhang, C.-M. Zhang, and Q. Wang, Optics letters 44, 1468 (2019).
- [74] X.-Y. Zhou, C.-H. Zhang, C.-M. Zhang, and Q. Wang, Physical Review A 99, 062316 (2019).
- [75] M. Minder, M. Pittaluga, G. Roberts, M. Lucamarini, J. Dynes, Z. Yuan, and A. Shields, Nature Photonics p. 1 (2019).
- [76] Y. Liu, Z.-W. Yu, W. Zhang, J.-Y. Guan, J.-P. Chen, C. Zhang, X.-L. Hu, H. Li, T.-Y. Chen, L. You, et al., arXiv preprint arXiv:1902.06268 (2019).
- [77] S. Wang, D.-Y. He, Z.-Q. Yin, F.-Y. Lu, C.-H. Cui, W. Chen, Z. Zhou, G.-C. Guo, and Z.-F. Han, arXiv preprint arXiv:1902.06884 (2019).
- [78] X. Zhong, J. Hu, M. Curty, L. Qian, and H.-K. Lo, arXiv preprint arXiv:1902.10209 (2019).
- [79] X.-T. Fang, P. Zeng, H. Liu, M. Zou, W. Wu, Y.-L. Tang, Y.-J. Sheng, Y. Xiang, W. Zhang, H. Li, et al., arXiv preprint arXiv:1908.01271 (2019).
- [80] S. Pirandola, R. Laurenza, C. Ottaviani, and L. Banchi, Nature communications 8, 15043 (2017).
- [81] J. Müller-Quade and R. Renner, New Journal of Physics 11, 085006 (2009).
- [82] R. König, R. Renner, A. Bariska, and U. Maurer, Physical Review Letters 98, 140502 (2007).
- [83] M. Tomamichel, C. C. W. Lim, N. Gisin, and R. Renner, Nature communications 3, 634 (2012).
- [84] R. Renner, Ph.D. thesis, SWISS FEDERAL INSTITUTE OF TECHNOLOGY ZURICH (2005).
- [85] H. Chernoff et al., The Annals of Mathematical Statistics 23, 493 (1952).